JMEPEG (2009) 18:939–946
DOI: 10.1007/s11665-008-9321-6

1059-9495/$19.00

Investigation of Contact Fatigue of High Strength Steel Gears Subjected to Surface Treatment

L. Dimitrov, D. Michalopoulos, Ch. Alk. Apostolopoulos, and T.D. Neshkov

(Submitted July 27, 2008)

In this paper the contact fatigue resistance of gearwheel teeth, subjected to shot-peening treatment, was investigated experimentally and analytically. The main objective was the evaluation and prediction of fatigue crack initiation, propagation, direction, and rate. A specially designed experimental rig was used to test a number of spur gears with the following characteristics: (a) unhardened, thermally untreated unpeened surfaces, (b) thermally treated unpeened surfaces, (c) unhardened peened surfaces, and (d) thermally treated peened surfaces. The theoretical model assumed initiation and propagation of surface cracks of gears operating in the elastohydrodynamic lubrication regime while loading was due to simultaneous rolling and sliding. Finite element modeling was used for the calculation of the stress field at the gear teeth. Comparison of the experimental and analytical results showed considerable improvement in the contact fatigue strength of thermally treated gear teeth and especially those that underwent shot peening, which increased surface durability. The residual stresses induced by shot peening are mainly effective in stopping microcrack propagation. When shot peening is applied on thermally untreated gear teeth surface, it increases the contact fatigue life of the material by 17% at 7×10^5 loading cycles. If shot peening is applied on carburized gear teeth surfaces, it increases the surface fatigue life by approximately 8% at 10^6 cycles. Contact fatigue and eventual pitting are treated as a normal consequence of the operation of machine elements. To study this failure process different types of testing machines have been designed. The purpose of this paper is the presentation and evaluation of a new design experimental rig for studying contact fatigue damage of gear teeth subjected to different load patterns.

Keywords contact fatigue, residual stress, shot peening, surface treatment, thermal treatment

1. Introduction

Mechanical components such as gears, shafts, cams, and springs, are subjected to static and to rapidly fluctuating cyclic or periodic loads causing cyclic stresses. Under these conditions, the parts fail due to contact fatigue, at a stress lower than what failure would have occurred under static loading. Contact fatigue damage is very complicated, and during simulation the type of material, the geometry involved, the mode of lubrication, and the size should be considered.

Surface durability of gear teeth very often limits the size of gear transmission, and therefore, it is important to have reliable information about the surface fatigue life of the material, obtained experimentally (Ref 1-4). Several test rig designs are available for evaluating the surface fatigue life of gear teeth (Ref 1, 2, 4-9).

Tests made on real gearwheel specimens are listed in the literature (Ref 1, 2, 7-9). Their design is based on the "four-square" principle (known also as "back-to-back") or by the use of linear scheme (Ref 1, 2, 7-9). A popular design of gear fatigue test apparatus is the rig used by NASA Glenn Research Center, based on the "four-square" principle.

Tests are made on roller to roller type test rigs (Ref 4-6, 10) during which the effect of different surface treatments over the surface durability are examined. The main failure modes for gear teeth are wear, scuffing, micropitting, and pitting.

Wear occurs in new gears during running-in and during start-ups and shut-downs where asperities interact. Figure 1 shows the typical wear process of gear teeth (Ref 11).

Scuffing is considered as localized damage caused by the occurrence of solid-phase welding between sliding gear flanks, due to excessive heat generated by friction, and it is characterized by the transfer of material between sliding tooth surfaces. This condition occurs during metal-to-metal contact between gear teeth and due to the removal of the protective oxide layer of the gear surfaces. Figure 2 shows a typical scuffing condition of gear teeth.

Micropitting, shown in Fig. 3, is a fatigue failure of the surface where, predominantly in the areas of negative sliding below the pitch circle, microcracking leads to material break out. The size of these defects is approximately 10-20 µm deep by 25-100 µm long and 10-20 µm wide.

Pitting, shown in Fig. 4, is a typical failure of gear teeth operating under elastohydrodynamic lubrication (EHDL) and originating from surface breaking or a subsurface crack. Surface cracks are caused during machining or due to some hard particle, that is found in the lubricant, while subsurface cracks originate from inclusions in the gear material.

L. Dimitrov and **T.D. Neshkov**, Department of Mechanical Engineering, Technical University of Sofia, Sofia 1000, Bulgaria; and **D. Michalopoulos** and **Ch. Alk. Apostolopoulos**, Department of Mechanical Engineering and Aeronautics, University of Patras, Patras 26500, Greece. Contact e-mail: mixalop@mech.upatras.gr.

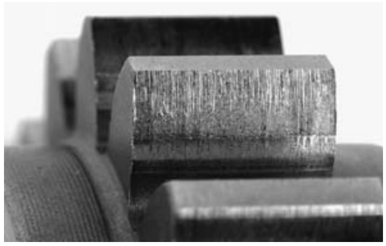

Fig. 1 Wear of a gear tooth

Fig. 2 Scuffing of gear teeth

Fig. 3 Micropitting of gear teeth

Fig. 4 Pitting of gear teeth flanks

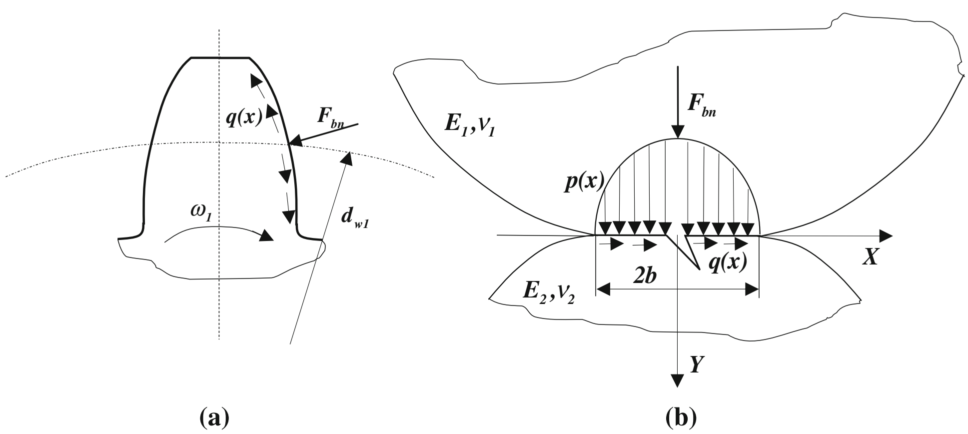

Fig. 5 Loading of gear teeth in the contact zone

Results from roller to roller tests are mostly utilized to select the material of mechanical components and for evaluation of different surface treatments over the surface durability. Tests on real components give more reliable information and present day practice shows the increasing use of such experimental results. The surface durability of gear teeth is examined experimentally on real specimens because of the complicated geometry and loading of gear teeth, rolling, and sliding, whose magnitude and sign changes along the tooth during engagement (Ref 11). In most material failures, tensile stresses appear to be the common mode and the material surface is stretched or pulled apart, thus leading to microscopic surface cracking and macroscopic-scale pitting or spalling.

Shot peening is a cold working surface treatment during which the surface of a part is bombarded with small spheres of different materials, known as shot. This process enhances the fatigue life or load range of mechanical parts by work hardening of their surface and creating residual compressive stresses. It is harmless to the environment while the performance and reliability of the subject elements are upgraded. It is used extensively on mechanical elements of complex geometry such as gears, shafts, springs, turbine, and compressor blades. Shot peening is more of an empirical art rather than scientific process and operator experience is important for the integrity of the end result. A few attempts have been made to quantitatively predict the effectiveness of the process in practical applications. In addition, the parameters involved (shot size, material, velocity, and the target component) are chosen according to the operator experience and sensitivity rather than following methods and standards developed analytically. Shot peening intensity is expressed in degrees Almen, a unit that adapts well to industrial applications but cannot allow one to get a direct relationship with the induced range of residual stress, which produces changes in the mechanical performance of the pieces under treatment (Ref 12, 13).

2. Contact Zone Loading of Gear

Gear teeth subjected to repeated Hertzian loading in the contact zone fail mostly due to contact fatigue, as illustrated in Fig. 1. When teeth come into contact, they act upon one another with normal force F_{bn}, which is distributed in the contact area $2b$ as surface pressure $p(x)$ (Fig. 5b). During engagement, gear teeth slide upon one another and a force $q(x)$ appears acting in the direction opposite to the sliding velocity, as shown in Fig. 5(a). Surface Hertzian contact pressure together with the friction loading on the surface layers leads to the development and propagation of surface-initiated cracks (Ref 14, 15).

A special case of gears operating in oil is the EHDL in the contact zone. The Hertz pressure distribution for the case of EHDL is illustrated in Fig. 6.

3. Experimental Procedure

Figure 7 shows the gear contact fatigue test rig used in this investigation, consisting of an electric motor driving two identical gear boxes connected with four universal joints so as to avoid additional loads in the assembly and a loading coupling. Each one of the two gear boxes contains one pair of identical gears and is connected by their input and output shafts so that two identical gear pairs may be examined simultaneously. This particular test rig design uses the so-called four-square principle of applying test loads. Thus, the input drive needs only to overcome the frictional losses in the system. Figure 8 shows the tested gearwheels.

Figure 9 shows the specially designed loading coupling by which torque may be transmitted to the test gears prior to start-up. To achieve the required torque, the two coupling hubs are rotated in opposite directions with the help of two pin-face adjustable spanner wrenches. The loaded torque is set by a torque indicating wrench. Then the two parts of the coupling are fixed together by pins. This design of loading coupling allows for achieving different loading torques. It could be accomplished by fixing the two coupling flanges at different angles, so that the holes on one of the flanges are drilled with different pitches. This torque is transmitted through the test gearwheels, loading the teeth to the desired contact or Hertz stress level gradually.

Preloading is responsible for the early damage of carburized and hardened toothflanks. Shot peening was applied to improve the gear teeth contact performance, since it induces inside the surface layers of the material a compressive residual stress field, which can delay the damage process caused by the repetition of contact cycles. The treatment improved the fatigue level of the gear teeth surface resistance.

The operating speed for the tests conducted was 3000 rpm resulting in a pitch-line velocity of approximately 1.35 m/s, while the lubricant was supplied to the inlet mesh, by a pump,

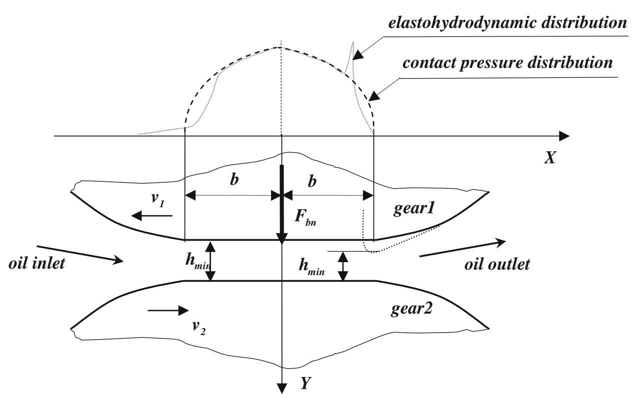

Fig. 6 Hertz contact pressure distribution and Elastohydrodynamic distribution in the contact of gear teeth

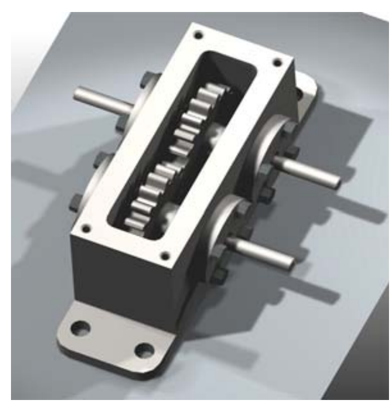

Fig. 8 Photograph of the tested gear box

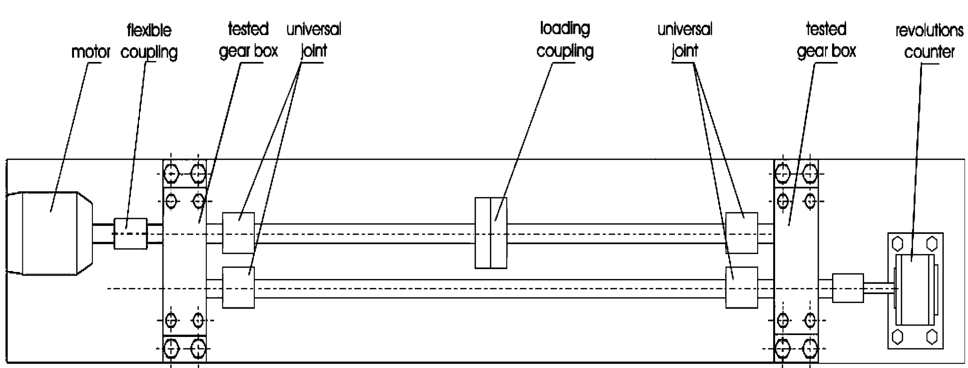

Fig. 7 Schematic diagram of the gear fatigue test rig

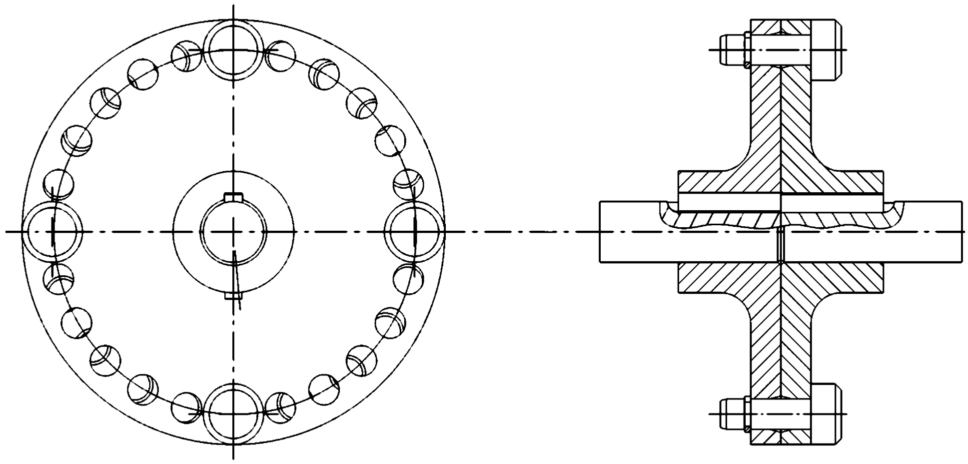

Fig. 9 Loading coupling

at approximately 1.5-3.0 cm^3/min at a temperature of 331.15 K, which was monitored at regular time intervals, and the maximum temperature reached at the maximum load was 338.15 K. It was calculated that at this speed the EHDL of gear teeth was achieved. A revolution counter was used to count the loading cycles, and thermocouples were fitted in each gearbox, which monitored the oil temperature and shut-off the motor in case of overheating. The test lubricant was mineral oil with kinematic viscosity index at 373.15 K of 19.5 mm^2/s and density of 0.901 g/cm^3, at temperature of 293.15 K. The stresses developed on the gear teeth were calculated using Finite Elements method.

4. Specification of the Gear Tested

The tests were conducted with four groups of identical gears, produced from the same material, ISO steel C45, corresponding to SAE (AISI) 1045 steel, which is a relatively inexpensive material and one of the most commonly used in ordinary practice (Ref 16). Tables 1 and 2 show the percent composition and mechanical properties of the gear steel used.

All tested gears had involute teeth, corresponding to ISO basic rack tooth profile (Ref 17). The test gear nomenclature is described in Table 3.

Surface roughness of the gear teeth contacting surfaces (involute surfaces) was R_a = 1.25. The examined gears were divided into groups corresponding to their surface treatment as follows:

Group A—unhardened, thermally untreated gear teeth, without shot peening. The normal core hardness was HB 230.

Group B—thermally treated gear teeth, without shot peening. The samples were carburized to a surface carbon content of 0.8% and a case depth of approximately 1.0 mm. After treatment a case hardness of Rockwell C (HRC) 59 was achieved.

Group C—unhardened, shot-peened gear teeth. Gears were shot peened after finish grinding. The shot-peening intensity was expressed by Almen degrees and for gears in this group was about 0.21 A.

Table 1 Percentage chemical composition of the gear steel tested

C	Si	Mn	P	S
0.45	0.25	0.60	0.045	0.045

Table 2 Mechanical properties of the gear steel tested

Ultimate tensile strength, σ_u, MPa	Yield strength σ_y, MPa	Modulus of elasticity, E, GPa	Hardness, HB, BHN
610	360	210	230

Table 3 Gear nomenclature

Parameter	Symbol	Unit	Value
Module	m	mm	3
Number of teeth	z	···	18
Pressure angle	α	deg	20°
Helix angle	β	deg	0°
Pitch diameter	d	mm	54.0
Shift coefficient	x	mm	0
Addendum diameter	d_a	mm	60.0
Dedendum diameter	d_f	mm	46.5
Face width	b	mm	12.0

Group D—thermally treated, shot peened gear teeth. After carburization of gears they were shot peened to Almen intensity of 0.36 A.

5. Test Procedure

In all experiments a torque of 3 N m was initially locked in the system and the gears were run for about 15 min, after which the lubricant was changed. After that the torque was raised to the required torque level and the gears were run at rated speed. Gears were tested for Hertzian contact pressure between the teeth at 600, 700, 800, 900, 1000, and 1100 MPa. The loading torque needed for achieving the required allowable contact pressure was calculated according to the ISO relationship for surface durability (Ref 18):

$$\sigma_H = Z_E \cdot Z_H \cdot Z_\varepsilon \sqrt{\frac{2T}{b_1 d^2} \frac{u+1}{u} K_A \cdot K_V \cdot K_{H\alpha} \cdot K_{H\beta}} \leq \sigma_{HP} = \frac{\sigma_{H\,lim} \cdot Z_N}{S_{H\,min}} \qquad \text{(Eq 1)}$$

For the experiments, it was assumed that $Z_N = 1.0$ and the contact stress safety factor $S_{H\ min} = 1.0$.

The required torque (T) was imposed into the system by the use of the loading coupling (Fig. 9). Angles (φ) to which the coupling flanges should be rotated with respect to each other were calculated by Eq 2 (Ref 19).

$$\varphi = \int_0^x \frac{T \cdot dx}{G \cdot J} \qquad \text{(Eq 2)}$$

During the tests, the rig was stopped at intervals of 100,000 cycles and the teeth were inspected for pit formation using a magnifying glass. The experiments in which no failure was observed even after running for 60,00,000 cycles were terminated.

Table 4 Experimentally obtained data

Surface contact stress, MPa	Number of cycles to breakage			
	Group A	Group B	Group C	Group D
1100	8.0×10^4	6.1×10^5	1.9×10^5	1.8×10^5
1000	1.2×10^5	1.0×10^6	2.5×10^5	1.1×10^6
900	2.0×10^5	1.3×10^6	3.2×10^5	1.7×10^6
800	2.8×10^5	1.8×10^6	4.6×10^5	2.2×10^6
700	3.9×10^5	2.3×10^6	7.4×10^5	...
600	6.6×10^5	...	...	...

6. Experimental Results

The aim of the experiments was to determine the number of cycles until the first evidence of surface fatigue. It was considered that pitting occurred when the size of micropitts exceeded 40 μm (Ref 20). Two sets of gears were tested in each experiment under identical conditions. In each group, 12 identical gears were tested. The results from the tests are shown in Table 4.

Figure 10 illustrates the experimentally obtained results included in Table 4, drawn in semilogarithmic graph, for the four groups of gears, which are typical fatigue stress-life curves. Similar results for pitting-spalling fatigue failure but for other types of steels and loaded in similar conditions could be found in the literature (Ref 6, 20-24).

7. Analytical Results

A computer model based on fracture mechanics was devised to determine the fatigue of mechanical components, and it is applied by the authors for the calculation of contact fatigue life of gears. It simulates the initiation and propagation of surface cracks of gears operating in oil. In the development of the model, the following assumptions were made:

(a) Both rolling and sliding action took place.
(b) EHDL regime was considered.
(c) Mutual interaction between surfaces resulted in crack initiation.
(d) The gear teeth material was isotropic and homogeneous.
(e) The contacting surfaces were absolutely smooth and without any surface treatment and residual stresses.
(f) Increased intensity of shot peening improved the performance of gear teeth.

Shot peening has a beneficial effect in stopping microcrack growth but not in preventing initiation.

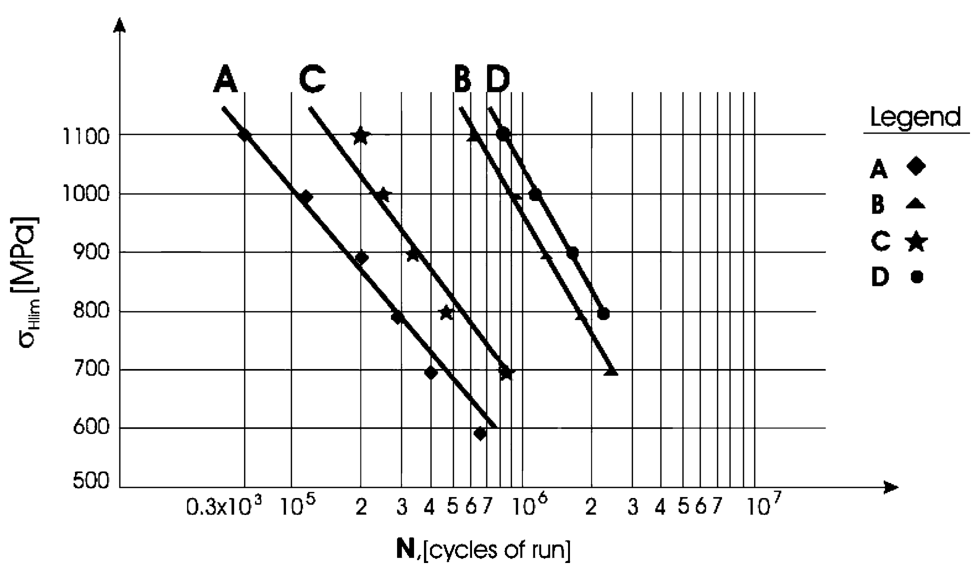

Fig. 10 Contact fatigue life curves of examined gears

Table 5 Results from experiments (E) and simulation (S)

Surface contact pressure, MPa	Number of cycles to failure							
	A_E	A_S	B_E	B_S	C_E	C_S	D_E	D_S
1100	8.00E + 04	6.83E + 04	6.10E + 05	6.20E + 05	1.90E + 05	2.13E + 05	1.80E + 05	1.97E + 05
1000	1.20E + 05	1.20E + 05	1.00E + 06	9.27E + 05	2.50E + 05	2.64E + 05	1.10E + 06	1.26E + 06
900	2.00E + 05	1.78E + 05	1.30E + 06	1.25E + 06	3.20E + 05	3.24E + 05	1.70E + 06	1.85E + 06
800	2.80E + 05	2.70E + 05	1.80E + 06	1.66E + 06	4.60E + 05	4.59E + 05	2.20E + 06	2.36E + 06
700	3.90E + 05	3.88E + 05	2.30E + 06	2.20E + 06	7.40E + 05	6.95E + 05		3.16E + 06
600	6.60E + 05	6.45E + 05		3.61E + 06		1.32E + 06		4.63E + 06

The two-dimensional model was developed using Finite Element analysis and simulated a meshing cycle of the gearwheels. The gear contact service life (N) shown in Eq 3 was divided in the crack phase initiation (N_i) and the crack phase propagation (N_p).

$$N = N_i + N_p \quad \text{(Eq 3)}$$

The number of cycles to failure and crack initiation was evaluated by Coffin-Manson relation (Eq 4), which includes the material parameters σ'_f, fatigue strength coefficient; ε'_f, fatigue ductility coefficient; b, strength exponent, and c, fatigue ductility exponent. $\Delta\varepsilon$, $\Delta\varepsilon_e$, and $\Delta\varepsilon_p$ are the total, elastic, and the plastic strain amplitudes, respectively.

$$\frac{\Delta\varepsilon}{2} = \frac{\Delta\varepsilon_e}{2} + \frac{\Delta\varepsilon_p}{2} = \frac{\Delta\sigma}{2E} + \varepsilon'_f\left(\frac{\Delta\sigma}{2\sigma'_f}\right)^{\frac{1}{n'}} = \frac{\sigma'_f}{E}(2N_i)^b + \varepsilon'_f(2N_i)^c \quad \text{(Eq 4)}$$

Crack initiation threshold, α_{th}, for each material was determined from Eq 5, where ΔK_{th} is stress intensity gradient (Ref 25, 26).

$$a_{th} = \frac{1}{\pi}\left(\frac{\Delta K_{th}}{2\sigma_s}\right)^2 \quad \text{(Eq 5)}$$

On the basis of the model for crack growth, Paris equation was used as follows.

$$\frac{da}{dN_p} = C[\Delta K(a)]^m \quad \text{(Eq 6)}$$

where $\Delta K(a)$ is the effective stress intensity factor, which for short cracks can be written as

$$\Delta K = F_{IS} \cdot K_t \cdot \Delta\sigma \cdot \sqrt{\pi \cdot a} \quad \text{(Eq 7)}$$

The coefficient F_{IS} in Eq 7 accounts for short cracks interaction effects, while K_t is a stress concentration factor. $\Delta\sigma = (\sigma_{max} - \sigma_{min})/2$ is the applied stress range and α is the crack length.

In the proposed model, the effect of crack interaction is taken into account. This effect becomes significant when the asperity density is high and the distance between cracks is relatively small. For short crack case in the model, the following equation for the crack interaction factor is used [27]:

$$F_{IS} = 1.2 - 0.293\frac{2a}{2a+h}\left[1 - \left(1 - \frac{2a}{2a+h}\right)^4\right] \quad \text{(Eq 8)}$$

where h is the distance between adjacent cracks.

The stress intensity factors K_I and K_{II}, for crack propagation were determined from Eq 7 and 8.

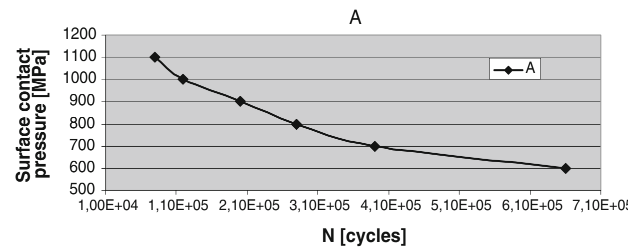

Fig. 11 Surface contact pressure behavior versus number of cycles for Group A

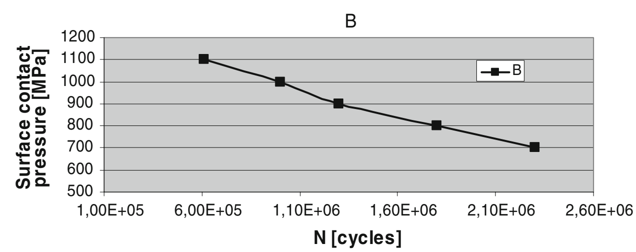

Fig. 12 Surface contact pressure behavior versus number of cycles for Group B

$$K_I = \frac{G}{k+1}\sqrt{\frac{2\pi}{L}}[4(v_2 - v_4) + (v_5 - v_3)] \quad \text{(Eq 9)}$$

$$K_{II} = \frac{G}{k+1}\sqrt{\frac{2\pi}{L}}[4(u_2 - u_4) + (u_5 - u_3)] \quad \text{(Eq 10)}$$

The crack propagation angle θ is determined from:

$$\theta_i = 2\left[\tan\left(\frac{1}{4}\frac{K_I}{K_{II}} \pm \sqrt{\left(\frac{K_I}{K_{II}}\right)^2 + 8}\right)\right]^{-1} \quad \text{(Eq 11)}$$

Stress determination in a crack tip is made by the use of finite element analysis, and calculation of stress intensity factors and number of cycles is accomplished by the use of MATLAB program.

Table 5 displays a comparison between experimental and analytical results.

Figures 11-14 show the experimental results comprising the contact pressure versus number of cycles for each group of gears tested, A, B, C, and D, while Fig. 15 shows a summary of all tests.

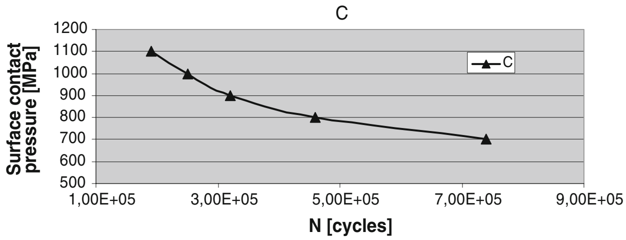

Fig. 13 Surface contact pressure behavior versus number of cycles for Group C

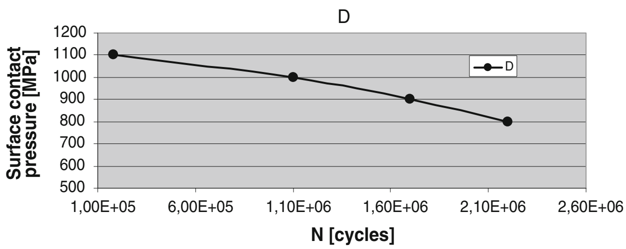

Fig. 14 Surface contact pressure behavior versus number of cycles for group D

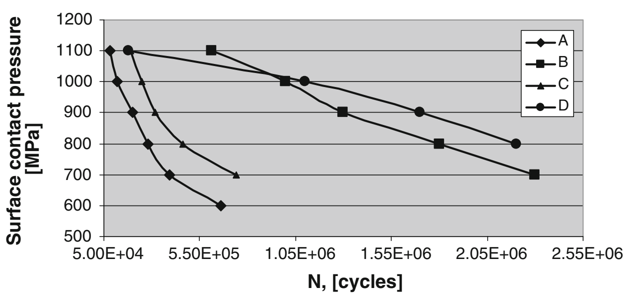

Fig. 15 Summary of surface contact pressure behavior versus number of cycles for Groups A, B, C, and D

8. Conclusions

A test rig design, based on the "four-square principle," was used for the examination of gear teeth surface durability. This rig could be used for the evaluation of gear teeth contact fatigue life for different gear materials, for gear teeth with different surface treatment, and for different lubricants.

The surface contact characteristics of thermally untreated, thermally treated, and shot-peened gears made of ISO 45 steel were studied and their S-N curves were obtained. These curves show improvement in contact fatigue strength of thermally treated gear teeth in contrast to unhardened teeth. The best characteristics were identified for thermally treated gear teeth that had been subjected to shot peening, which was found to increase gear teeth surface durability. When applied on thermally untreated gear teeth surfaces, the contact fatigue life is increased by approximately 17% at 7×10^5 cycles. If applied on carburized gear teeth surface, shot peening increases surface fatigue life by approximately 8% at 10^6 cycles.

Simulation showed that the number of cycles until crack initiation is much higher (7.44 times) than that for the propagation of cracks until the appearance of pitting.

The propagation of contact fatigue cracks grows slowly when going deep inside the material (about 70% of its life) while it grows very fast up to the surface.

References

1. T.L. Krantz, M.P. Alanou, H.P. Evans, and R.W. Snidle, Surface Fatigue Lives of Case-Carburized Gears with an Improved Surface Finish, *J. Tribol.*, 2001, **123**, p 709–716
2. D.P. Townsend and E.V. Zaretsky, Effect of Shot Peening on Surface Fatigue Life of Carburized and Hardened AISI 9310 Spur Gears, NASA Technical Paper No. 2047, 1982
3. M. Guagliano, E. Riva, and M. Guidetti, Contact Fatigue Failure Analysis of Shot-Peened Gears, *Eng. Fail. Anal.*, 2002, **9**, p 147–158
4. W. Widmark and A. Melander, Effect of Material, Heat Treatment, Grinding and Shot Peening on Contact Fatigue Life of Carburised Steels, *Int. J. Fatigue*, 1999, **21**(4), p 309–327
5. M.F. Frolish, D.I. Fletcher, and J.H. Beynon, A Quantitative Model for Predicting the Morphology of Surface Initiated Rolling Contact Fatigue Cracks in Back-Up Roll Steels, *Fatigue Fract. Eng. Mater. Struct.*, 2002, **25**(11), p 1073–1086
6. A. Yoshida and M. Fujii, Influence of Soft Surface Modification on Rolling Contact Fatigue Strength of Machine Elements, *Tribol. Int.*, 2002, **35**(12), p 837–847
7. D. Nelias, Role of Inclusions, Surface Roughness and Operating Conditions on Rolling Contact Fatigue, *Trans. ASME*, 1999, **121**, p 240–251
8. Y. Ding and N.F. Rieger, Spalling Formation Mechanism for Gears, *Wear*, 2003, **254**(11), p 1307–1317
9. B.R. Höhn and K. Michaelis, Influence of Oil Temperature on Gear Failures, *Tribol. Int.*, 2004, **37**, p 103–109
10. B.Y. Choi and C.S. Lee, Characteristics of Rolling Contact Fatigue of Steels Produced by Thermomechanical Processing, *J. Mater. Sci.*, 2001, **36**(21), p 5237–5243
11. P.J.L. Fernandes and C. McDuling, Surface contact Fatigue in Gears, *Eng. Fail. Anal.*, 1997, **2**, p 99–107
12. K.J. Marsh, *Shot Peening: Techniques and Applications,* EMAS, Warrington, UK, 1993
13. R. Herzog, W. Zinn, B. Sholtes, and H. Wohlfahrt, The Significance of Almen Intensity for the Generation of Shot Peening Residual Stresses, *Proceedings of the VI International Conference on Shot Peening,* San Francisco, 1996, p 270–281
14. K.L Johnson, *Contact Mechanics*, Cambridge University Press, Cambridge, 2001
15. V.M. Aleksandrov, *Three-Dimensional Contact Problems*, Kluwer Academic Publishers, Boston, MA, 2001
16. ISO 683-1, Heat-Treatable Steels, Alloy Steels and Free-Cutting Steel. Direct-Hardening Unalloyed and Low Alloyed Wrought Steel, 1987
17. ISO 53, Cylindrical Gears for General and Heavy Engineering—Standard Basic Rack Tooth Profile, 1998
18. ISO 6336-2: Calculation of Load Capacity of Spur and Helical Gears, Calculation of Surface Durability (Pitting), 2005
19. www.prista-oil.com, 2008
20. J.M Gere and S.P. Timoshenko, *Mechanics of Materials*, Chapman & Hall, New York, 1991
21. T.E. Tallin, *Failure Atlas for Hertz Contact Machine Elements*, 2nd ed., ASME Press, New York, 1999
22. T. Susuki, K. Ogawa, and Sh. Hotta, Experimental Analysis and Life Prediction of Pitting Failures for Carburized Gear Material, *ASME Design Engineering Technical Conference, 8th International Power Transmission and Gearing conference,* September 10-13, 2000 (Baltimore, Maryland), p 163–169
23. M. Girish, M. Mayuram, and S. Krishnamurthy, Influence of Shot Peening on the Surface Durability of Thermomechanically Treated En24 Steel Spur Gears, *Tribol. Int.*, 1997, **30**(12), p 865–870

24. D. Michalopoulos, N. Aspragathos, and A.D. Dimarogonas, Fatigue Damage of Gear Teeth in Speed Reducers Moving Heavy Rotors, *Trans. ASME*, 1987, **109**, 196
25. T.L. Anderson, *Fracture Mechanics. Fundamentals and Applications*, CRC Press, London, 1995, ISBN 0849342600
26. S. Suresh, *Fatigue of Materials,* 2nd ed., Cambridge University Press, Cambridge, 2004, ISBN 0521570468
27. A. Andrews and H. Sehitoglu, A Computer Model for Fatigue Crack Growth from Rough Surfaces, *Int. J. Fatigue*, 2002, **22**(2), p 619–630